Acid resistance of alkali-activated materials: recent advances and research needs

Gregor J.G. Gluth[1],*, Cyrill Grengg[2], Neven Ukrainczyk[3], Florian Mittermayr[4], Martin Dietzel[2]

[1] Division 7.4 Technology of Construction Materials, Bundesanstalt für Materialforschung und -prüfung (BAM), Unter den Eichen 87, 12205 Berlin, Germany
[2] Institute of Applied Geosciences, Graz University of Technology, Rechbauerstraße 12, 8010 Graz, Austria
[3] Institute of Construction and Building Materials, Technical University of Darmstadt, Franziska-Braun-Strasse 3, 64287 Darmstadt, Germany
[4] Institute of Technology and Testing of Building Materials, Graz University of Technology, Inffeldgasse 24, 8010 Graz, Austria

Abstract

Cementitious materials are frequently applied in environments in which they are exposed to acid attack, e.g., in sewer systems, biogas plants, and agricultural/food-related industries. Alkali-activated materials (AAMs) have repeatedly been shown to exhibit a remarkably high resistance against attack by organic and inorganic acids and, thus, are promising candidates for the construction and the repair of acid-exposed structures. However, the reaction mechanisms and processes affecting the acid resistance of AAMs have just recently begun to be understood in more detail. The present contribution synthesises these advances and outlines potentially fruitful avenues of research. The interaction between AAMs and acids proceeds in a multistep process wherein different aspects of deterioration extend to different depths, complicating the overall determination of acid resistance. Partly due to this indistinct definition of the 'depth of corrosion', the effects of the composition of AAMs on their acid resistance cannot be unambiguously identified to date. Important parallels exist between the deterioration of low-Ca AAMs and the weathering/corrosion of minerals and glasses (dissolution-reprecipitation mechanism). Additional research requirements relate to the deterioration mechanism of high-Ca AAMs; how the character of the corroded layer influences the rate of deterioration; the effects of shrinkage and the bond between AAMs and substrates.

Keywords: Acid corrosion; Inorganic acids; Organic acids; Durability; Geopolymers

1 Introduction

In several applications and environments, concretes and other cementitious materials are exposed to aqueous solutions with low pH, *i.e.*, acid(ic) solutions; examples include sewer structures, cooling towers, areas of acid mine drainage, biogas plants, agricultural structures, and dairy plants. The exposure to acidic aqueous media often causes severe deterioration ('acid corrosion'), *i.e.*, degradation of the cementitious materials at a fast rate, which frequently leads to premature failure of structural elements and associated high expenses for temporary shutdown, repair, and/or replacement. For example, the annual rehabilitation expenses to maintain the wastewater infrastructure have been estimated to be 450×10^6 € and 85×10^6 £ in Germany and in the United Kingdom, respectively, and the costs for that purpose in the United States have been projected to be 390×10^9 \$ for a period of 20 years [1]. Moreover, the structures affected by acid attack often fulfil important societal tasks, such as energy production, food production, or as parts of the wastewater treatment and sewerage infrastructure. Because of this high economic and societal relevance, there is a continuous search for cementitious materials with a high resistance against acid attack ('acid resistance') [2].

A particularly promising class of materials in this regard are alkali-activated materials (AAMs), *i.e.*, cementitious materials produced by the alkaline activation of reactive (alumino)silicates. The phase assemblages and the properties of these materials differ widely, depending on the composition of the employed precursors and activators, and the curing conditions [3, 4]. An important influence is exerted by the CaO content of the precursors, with a low CaO content [Ca/(Si+Al) ≈ 0] leading to a sodium or potassium aluminosilicate (N-A-S-H or K-A-S-H) gel as the major reaction product (low-Ca AAMs; often referred to as 'geopolymers'), and a high CaO content [Ca/(Si+Al) ≈ 1] leading to a sodium- or potassium-substituted calcium aluminosilicate hydrate [C-(N-)A-S-H or C-(K-)A-S-H] gel (high-Ca AAMs); intermediate CaO contents are thought to lead to a mixture of these gels [3, 4]. Nevertheless, a high acid resistance has been reported, already decades ago, for low-Ca AAMs based on metakaolin or fly ash as well as for high Ca-AAMs based on ground granulated blast furnace slag (GGBFS) [5–8], and this has been confirmed in many subsequent studies (Table 1). This raises

*Corresponding authors: Gregor J.G. Gluth, gregor.gluth@bam.de

the questions why the acid resistance of well-designed AAMs is generally very high, compared to materials based on ordinary Portland cement (OPC), and whether the mechanisms that determine their acid resistance differ between individual AAMs.

Early studies of the acid attack of AAMs often used the change of mechanical strength, the mass loss or the visually determined deteriorated depth ('depth of corrosion') after acid exposure to evaluate the performance of the investigated materials, offering only limited insight into the underlying deterioration mechanisms. In recent years, however, a number of studies have applied more sophisticated analytical techniques, which led to new insights into the acid attack on AAMs and their acid resistance. The present Letter summarises important results from some of these studies to assess whether common features or significant differences can be identified, and outlines research questions and possible approaches to further advance our understanding of the acid resistance of AAMs. Additional factors that are relevant for the successful application of AAMs in acid-exposed structures, e.g., as repair materials, are briefly discussed.

Table 1. Acid resistance of alkali-activated materials (AAMs) compared to ordinary Portland cement (OPC)-based materials.

Reference	AAM precursor(s)	Acid	pH	Acid resistance relative to OPC[b]
Blaakmeer 1994 [5]	GGBFS/fly ash	H_2SO_4	1.0	++
Shi and Stegemann 2000 [7]	GGBFS	HNO_3	3.0	+
	GGBFS	acetic acid	5.0	+
	GGBFS	acetic acid	3.0	++
Fernandez-Jimenez *et al.* 2007 [10]	Fly ash	HCl	1.0	++
Montes and Allouche 2012 [57]	Fly ash (class F)	H_2SO_4	0.6	++
	Fly ash (class C)	H_2SO_4	0.6	++
	Metakaolin	H_2SO_4	0.6	+
Bernal *et al.* 2012 [58]	GGBFS	HCl	3.0	≈
	GGBFS	HNO_3	3.0	≈
	GGBFS	H_2SO_4	3.0	≈
	GGBFS	acetic acid	4.5	++
Koenig *et al.* 2017 [42]	GGBFS	organic acid mix	~3	+
	GGBFS/fly ash	organic acid mix	~3	++
	Fly ash	organic acid mix	~3	++
Aliques-Granero *et al.* 2017 [40]	GGBFS	H_2SO_4, 1 %	1.0[a]	≈ [c]
	GGBFS	H_2SO_4, 3 %	0.5[a]	≈ [c]
	GGBFS	H_2SO_4, 5 %	0.3[a]	≈ [c]
	Fly ash	H_2SO_4, 1 %	1.0[a]	≈
	Fly ash	H_2SO_4, 3 %	0.5[a]	++
	Fly ash	H_2SO_4, 5 %	0.3[a]	++
Li and Peethamparan 2018 [59]	GGBFS	acetic acid	3.2	++
	GGBFS	acetic acid	4.0	++
	Fly ash (class C)	acetic acid	3.2	++
	Fly ash (class C)	acetic acid	4.0	++
Ukrainczyk *et al.* 2019 [60]	Metakaolin	acetic acid	2.0	++
Khan *et al.* 2020 [17]	Fly ash/GGBFS	H_2SO_4, 1.5 %	0.8[a]	+
Ren *et al.* 2022 [35]	GGBFS/Fly ash	H_3PO_4	2.0	+

[a] pH value calculated from the given concentration of H_2SO_4.

[b] Two plus signs (++) indicate that a relevant parameter (thickness of corroded layer, mass loss, or decrease of compressive strength) was >50 % better than for OPC; one plus sign (+) indicates that a relevant parameter was between approx. 25 % and 50 % better than for OPC; ≈ indicates that the performance of AAM and OPC was similar.

[c] Dissolution/mass loss for OPC mortar; expansion and cracking for GGBFS-based AAM.

2 Sequence of acid attack and leached layer development

Already early studies found that the acid attack on AAMs involves the formation of a leached layer at the acidic solution–material interface that is almost completely depleted in alkali ions (Na or K, depending on the activator), Ca and Al. For example, Allahverdi and Škvára [9] reported significant leaching of Ca, Na, and Al from an GGBFS/fly ash-based AAM exposed to HNO_3, while the fraction of Si in the corroded layer was increased after exposure at all studied pH values (1, 2, and 3). Based on these results, they concluded that the mechanism of acid attack is the same at all three pH values, differing only in severity. Similarly, Fernandez-Jimenez et al. [10] found that after the exposure of a fly ash-based AAM to HCl the amorphous binder phase of the corroded AAM was depleted in Al and its amount apparently increased (increase of "the area of the amorphous halo" in X-ray diffraction patterns).

These early observations are in line with what is known about the dissolution of aluminosilicate minerals and glasses at acidic and circum-neutral pH in general [11–13]: First, leaching of non-framework cations, i.e., exchange of alkali ions (Na^+ or K^+) and Ca^{2+} for H_3O^+, occurs. This is followed by removal of Al from the aluminosilicate framework by hydrolysis and exchange of Al^{3+} for H_3O^+. Finally, if Si–O–Si bonds are present in the framework (i.e., if the Si/Al ratio of the framework is >1), hydrolysis of these latter bonds occurs, and the aluminosilicate is dissolved. This sequence relates to the subprocesses that occur at the molecular level, while on a macroscopic level these subprocesses occur simultaneously. It can thus be concluded that the acid attack on AAMs is not significantly different from the dissolution of other aluminosilicates, and related information from disciplines such as mineralogy and geochemistry can be applied to understand the acid resistance of AAMs.

The mechanical strengths of the leached layers of various AAMs exposed to HNO_3 or H_2SO_4 have been found to be comparatively low, as these layers could be removed with a wire brush installed on an electric drill [14]. Based on this observation, attention was drawn to the fact that mass loss is not always an appropriate measure of acid resistance, as the corroded layer may partly or wholly detach from the intact material in some cases and in others not (depending on the material and the exposure conditions) [14]. This has been accounted for in most of the more recent studies by using other parameters (e.g., corroded layer thickness) in addition to, or instead of, mass loss as measure of resistance. However, it is noted that a decreased mechanical strength of the corroded layer is not necessarily a problem if it is stable enough to create an effective diffusion barrier and, thus, protects the subjacent intact material (see below). Moreover, it was also found that the leached layer of AAMs after acid attack retains substantial mechanical strength [15, 16], indicating that it would be stable enough to withstand abrasion and other mechanical stresses.
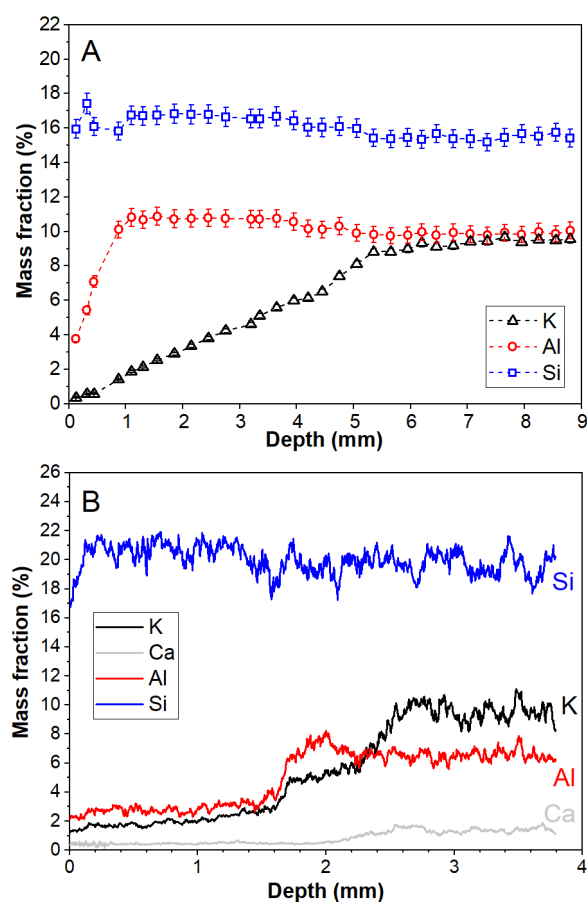

Figure 1. (A) Semi-quantitative concentration profiles [obtained by integrating energy-dispersive X-ray spectroscopy (EDS) mapping data] of K, Al and Si in a metakaolin-based AAM after exposure to acetic acid; the acid-exposed surface is shown left (depth = 0 mm). The respective depths to which K and Al are leached differ. (Data from [18].) **(B)** Concentration profiles [obtained by integrating wavelength-dispersive X-ray spectroscopy (WDS) mapping data] of K, Ca, Al and Si in a metakaolin-based AAM after exposure to biogenic sulfuric acid in a sewer system. The respective depths to which K and Al are leached differ. (Data from [21].)

Since the leached layer is depleted in alkali and Ca ions, its pH is generally lower than the pH of the intact material. The depth to which this neutralisation proceeds is often considerable, and samples with dimension of a few centimetres can be completely neutralised (pH < 10 as determined by spraying a phenolphthalein solution) within the period of a typical laboratory experiment (several weeks to few months) or field exposure (several months to few years), particularly if the material is a low-Ca AAM [15, 17]. For the comparatively simple case of deterioration of metakaolin-based AAMs in acetic acid, the leaching of alkali ions can be modelled using a single apparent diffusion coefficient for each combination of a specific material and leaching conditions [18, 19]. However, the inclusion of even low to moderate amounts of GGBFS in the precursors can significantly reduce the depth of the neutralised layer [15]. In addition, low neutralisation depths were also found in well-designed low-Ca AAMs [16], indicating the importance of material parameters such as porosity on alkali leaching. Further, it is important to note that the depth of the leached layer (as

determined with phenolphthalein or indicated by alkali ion concentration) is not necessarily identical to the depth of the layer in which complete Al removal and transformation of the materials has occurred [16, 18, 20, 21] (Fig. 1), which is related to the dependence of the mobility of the involved ions on pH. Thus, several definitions for the 'depth of corrosion' may be employed, and this must be considered when results from different studies are compared.

3 Dealumination and formation of a silica layer

As mentioned in the previous Section, the corroded layer of AAMs is generally found to be depleted in Al, usually determined by spatially resolved chemical analysis [scanning electron microscopy with energy-dispersive X-ray spectroscopy (SEM-EDS), electron probe microanalysis (EPMA) etc.]. In addition, several studies found that the X-ray diffraction (XRD) patterns of the corroded layer of low-Ca AAMs exhibits a broad hump centred at $d \approx 4.0$ Å ($2\vartheta \approx 22°$ for Cu Kα radiation), while the XRD patterns of the intact materials generally contain a broad hump centred at $d \approx 3.1$ Å ($2\vartheta \approx 29°$ for Cu Kα radiation) [16, 18, 22, 23] (Fig. 2). Comparison with the XRD patterns of silicate glasses with known chemical composition [24, 25] shows that this shift of the hump indicates the transformation of the Al-containing binder phase (N-A-S-H or K-A-S-H) to a virtually Al-free silica phase.
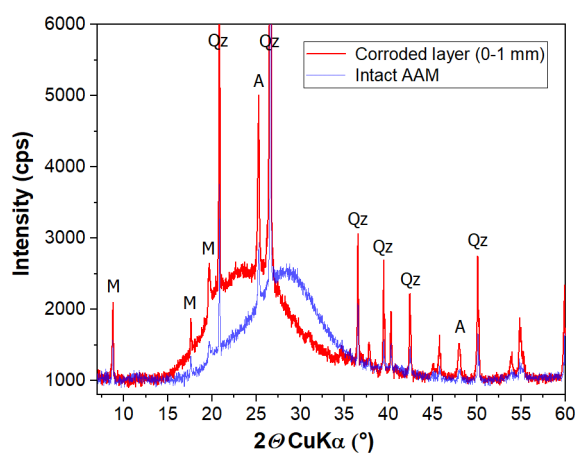

Figure 2. XRD patterns of an intact metakaolin-based AAM and the fully corroded layer of the AAM after exposure to acetic acid. A shift of the major hump in the pattern from ~29° to ~22°C indicates the formation of an Al-poor silica phase. Major peaks of crystalline impurities are labelled: M, muscovite/illite; A, anatase; Qz, quartz. (Data from [18].)

In line with these observations, Allahverdi and Škvára [26] demonstrated with ^{29}Si magic-angle spinning nuclear magnetic resonance (MAS NMR) spectroscopy that a partial conversion of Q^4(mAl) species to Q^4 species occurs during exposure of a GGBFS/fly ash-based AAM to HNO$_3$. [The 'Q-nomenclature' for SiO$_4$ tetrahedra [27] is used throughout this article. In this nomenclature system, the different SiO$_4$ sites are denoted by Q^n(mAl), where n indicates the number of oxygen-bridges to neighbouring SiO$_4$ and AlO$_4$ tetrahedra, and $m \leq n$ indicates the number of AlO$_4$ of these tetrahedra; for $m = 0$, the expression in parentheses is omitted.] Based on

this and additional spectroscopic data, they proposed a model of the acid attack with the following steps: (1) exchange of Ca and Na in the binder phase by H$^+$ or H$_3$O$^+$, (2) breaking of Si–O–Al bonds and release of Al, (3) reoccupation of the created vacancies in the aluminosilicate network by Si. The authors admitted that the source of Si for the reoccupation of vacancies remains obscure in their model. Moreover, the last step of their model is apparently in contradiction to the general mechanism, described above, which involves breaking of Si–O–Si bonds. However, the idea of a silica layer that forms solely by Al leaching appears to have been implicitly retained in some of the subsequent articles about acid attack on AAMs.

In recent publications, new details of the formation of the silica layer have been revealed and used to refine the model of the deterioration of AAMs caused by acid attack. ^{29}Si MAS NMR spectra of silica/sodium aluminate-based AAMs with and without 25 % GGBFS addition demonstrated the almost complete transformation of the Q^4(mAl) species of the binder phase to Q^3 and Q^4 units, and a comparison of their ^{1}H-^{29}Si cross-polarization (CP) MAS NMR spectra with published spectra of silica gels indicated that these units had formed through precipitation of a silica gel [16]. A subsequent study on the deterioration of metakaolin-based AAMs in sulfuric acid [22] confirmed these NMR results (Fig. 3) and demonstrated that (1) the absolute amount of SiO$_2$ in the corroded layer was higher than in the intact material, (2) the Si/Al ratio of the attacking solution was close to the Si/Al ratio of the material during the first hours of exposure, but then decreased to values close to zero, and (3) oxygen isotope exchange occurred between the corroding AAM and the acid solution. These data were interpreted as indicating a mechanism in which the dissolution of the binder phase is essentially congruent, and the formation of the silica layer occurs by precipitation of a hydrous silica gel (SiO$_2$·nH$_2$O) [22]. It has been described in the previous section that leaching of non-framework cations (mainly alkali ions) precedes the dissolution of the aluminosilicate framework; the term 'congruent' is used here to denote a mechanism in which breaking of Si–O–Al (and potentially Si–O–Si) bonds in the AAM releases monomeric and oligomeric silica species together with the Al into solution, as opposed to a mechanism where leaching of Al leaves behind a coherent silica framework.
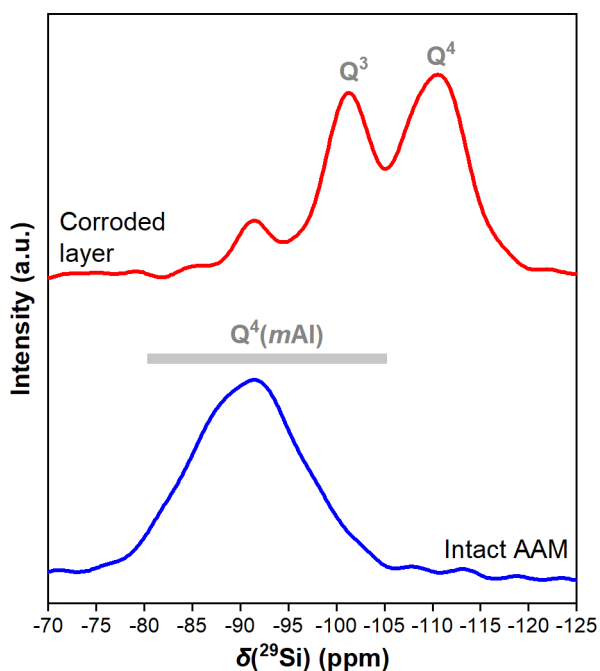
Figure 3. ^{29}Si MAS NMR spectra of an intact metakaolin-based AAM and the corroded layer of the AAM after exposure to sulfuric acid. The $Q^4(mAl)$ units with m = 1...4 in the intact material have mostly transformed to Q^3 and Q^4 units in the corroded layer. (Data from [22].)

Such a dissolution-reprecipitation mechanism is not only indicated by the above analytical results, but would also be predicted for the following reasons (see also the more detailed discussions in [16, 22, 28]): (1) The removal of Al from an aluminosilicate network with Si/Al ≤ 2, which is typical of the N-A-S-H and K-A-S-H gels of low-Ca AAMs, releases silica monomers and small silica oligomers, i.e., it leads to the almost complete destruction of the silicate network [13]. However, larger silica polymers may form as well, particularly at low pH and in the presence of bivalent cations [29]. (2) At low pH, the solubility of Al is high, while the solubility of Si is low, thus triggering the precipitation of silica gel if no complexing compound is present (Fig. 4).

It is further noted that a dissolution-reprecipitation mechanism has also been shown to be operative in the weathering/corrosion of aluminosilicate minerals and glasses at low and circum-neutral pH [30–32]. However, these studies found a steep chemical gradient between the corroded and intact regions of the materials, demonstrating that dissolution and precipitation occur within few nanometres or micrometres in the interface between these regions, while studies at a resolution required to confirm or reject this for AAMs are scarce (but see [22]). Thus, the spatial relationship between matrix dissolution and silica precipitation in AAMs needs to be studied in more detail to assess how similar the processes in minerals or glasses and AAMs are.
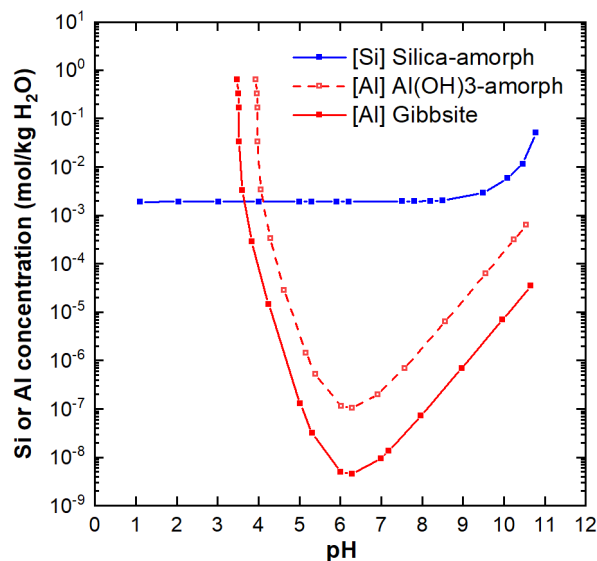

Figure 4. Solubilities of amorphous silica, amorphous $Al(OH)_3$, and gibbsite versus pH at 25°C, 1 bar. (Data computed with GEMS [61, 62], using the Cemdata18 database [63]; pH adjusted by addition of HCl/NaOH.)

Importantly, the study of mineral weathering [30] contended that the precipitated silica layer does not have a significant protective effect on the subjacent material, while the studies of glass corrosion [31, 32] concluded that the transport properties of the corroded layer (pore size and connectivity) control the overall deterioration kinetics, at least in the long term. As for acid attack on cementitious materials, a protective effect of the corroded layer has often been assumed. For example, Buvignier et al. [33] speculate that the formation of a low-diffusivity alumina layer during acid attack on hydrated calcium aluminate cement protects subjacent regions of the material. Shi and Stegemann [7] state that for alkali-activated slag, "inward movement of acid to the corrosion front […] becomes controlled by diffusion through this [calcium- and aluminium-leached] layer", and "the low lime content in activated-blast furnace slag […] pastes results in a dense silica gel protective layer." Finally, Lloyd et al. [14] find that "diffusion through the silica-rich product layer largely controls the rate of corrosion of an [AAM] binder." By analogy, it may be concluded that the corroded, silica-rich layer of low-Ca AAMs has a protective effect as well. However, the magnitude of this effect depends on the pore structure of the layer, and formation of expansive phases and cracking will exert an influence on it as well (see below).

Pertinent NMR data for high-Ca AAMs is not available, but a study by Wang et al. [34] employed NMR and other spectroscopic methods to study the deterioration of a nominally pure C-(N-)A-S-H gel in a 5 % H_2SO_4 solution (theoretical pH = 0.3). The ^{27}Al MAS NMR spectra showed that a fraction of the 4-coordinated Al (AlO_4) of the C-(N-)A-S-H gel had transformed to 6-coordinated Al (AlO_6) after exposure. The ^{29}Si MAS NMR spectrum exhibited prominent resonances at approx. −103 ppm and −112 ppm, which were not present in the spectrum of the C-(N-)A-S-H gel before acid attack. For a pure N-A-S-H gel that was also analysed in the study, ^{27}Al MAS NMR demonstrated a complete transformation of AlO_4

to AlO$_6$, and in the ^{29}Si MAS NMR spectra resonances at very similar chemical shifts (approx. −104 ppm and −112 ppm), clearly attributable to Q^3 and Q^4 species (because of the absence of AlO$_4$), respectively, were present after acid exposure. Thus, the results show that the transformation of C-(N-)A-S-H gel induced by acid attack bears important similarities with those of N-A-S-H gels, though it is unclear at present whether congruent dissolution of the C-(N-)A-S-H occurs.

4   Formation of secondary crystalline phases

Besides leaching and dissolution of the AAM, acid attack can also induce the formation of secondary phases, depending on the anion of the acid [2] and the composition of the AAM. The calcium salts of hydrochloric acid (HCl) and nitric acid (HNO$_3$) are highly soluble, *i.e.*, the precipitation of salts is usually not observed in studies using these acids, making the interpretation of the obtained results comparatively easy. The attack by sulfuric acid (H$_2$SO$_4$) is often more complex, as the sulfate ions tend to react with dissolved Ca and Al in the solution, potentially forming a number of different calcium sulfates (often gypsum, CaSO$_4$·2H$_2$O) and aluminium sulfates [e.g., alunite, KAl$_3$(SO$_4$)$_2$(OH)$_6$, and alum, KAl(SO$_4$)$_2$·12H$_2$O [22]]. In AAMs exposed to phosphoric acid (H$_3$PO$_4$), brushite (CaHPO$_4$·2H$_2$O) and other calcium phosphates as well as a sodium phosphate hydrate (Na$_2$HPO$_4$·12H$_2$O) have been observed [35], though the latter likely formed only during drying of the specimens. Several organic acids (e.g., acetic, lactic, citric, oxalic, and tartaric acid) are relevant in the context of acid attack on cementitious materials, as these can be produced by microorganisms in biogas plants as well as other agricultural and agri-food facilities [2, 36, 37]. Some of them, including acetic acid, form highly soluble calcium salts (*i.e.*, precipitation is not expected), while others lead to the precipitation of slightly soluble or insoluble calcium salts (e.g., Ca-oxalate), which in some cases may protect the subjacent material at least partially against further deterioration [36].

Early work of Allahverdi and Škvára [38, 39] on the deterioration of a GGBFS/fly ash-based AAM in H$_2$SO$_4$ found similar leaching profiles as for the corrosion in HNO$_3$; however, a calcium- and sulfur-rich layer was found to exist between the leached corroded layer and the intact material. Calcium for the formation gypsum was provided mainly by GGBFS in the studied material. The authors contended that the same corrosion mechanism as described above for HNO$_3$ was operative, but in addition gypsum formed in the pores and the cracks of the corroded layer, providing densification and protection for the subjacent material.

However, the precipitation of secondary mineral phases usually has a deleterious effect, mainly through expansion, associated crack formation and detachment of material. For example, Aliques-Granero *et al.* [40] observed that the formation of gypsum in a GGBFS-based AAM can lead to cracking and complete fragmentation of samples with dimensions of several centimetres when exposed to sulfuric acid with H$_2$SO$_4$ concentrations ≥3 %. In the study by Grengg *et al.* [22], various K/Al-sulfates and calcium sulfates were found in the corroded layers of low-Ca AAMs (Fig. 5). The

sulfate phases were mainly located in cracks, indicating that their precipitation can play an important role by inducing cracking and the associated ingress of acid even in materials with a low Ca content.
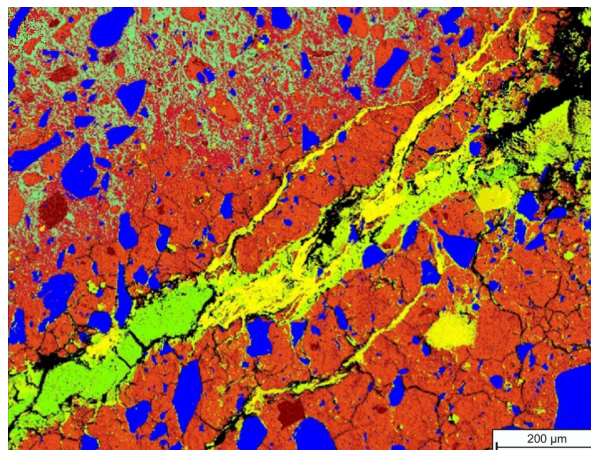

Figure 5. High-resolution phase distribution (obtained through phase calculations with XMapTool based on quantitative EPMA mappings) of a region in the transition zone between the corroded layer and the intact core of a metakaolin-based AAM after exposure to sulfuric acid (pH = 2) for 35 days at room temperature. The intact core of the specimen is located towards the top left of the image; the outer, exposed surfaces of the specimen are located towards the right and the bottom of the image. Several different sulfate phases are located in cracks. [Adapted from C. Grengg *et al.*, Cem Concr Res (2021) 142: 106373 [22], published under a Creative Commons license: https://creativecommons.org/licenses/by/4.0/; the label 'A' has been removed from the top left corner of the original image and the image cropped.]

5   Influence of AAM composition on acid resistance

Because of the wide range of employed precursors and activators of AAMs as well as the different parameters used to evaluate their acid resistance (Sections 1 and 2), the influence of AAM composition on their acid resistance is difficult to disentangle. The situation is further complicated by the fact that the relative performance of AAMs differs depending on the attacking acid (Table 1), at least partly due to the effect of secondary crystalline phase formation (Section 4). However, the below examples may serve to demonstrate some possible effects of the composition of AAMs on their acid resistance.

Lloyd *et al.* [14] observed a significant increase of the sulfuric acid resistance (decrease of the depth of corrosion) of AAMs with increasing GGBFS fraction, the other precursor being Class F fly ash. For the AAM produced from 100 % GGBFS, the formation of gypsum and associated cracks were observed in the corroded layer, yet its depth of corrosion was the lowest, *i.e.*, the GGBFS-based AAM possessed the highest acid resistance, despite the formation of a corroded layer with a weak protective effect. The authors assigned these observations to a decreasing permeability of the materials with increasing GGBFS fraction, caused by the formation of more binder phase including C-(N-)A-S-H. Confirming this

assignment, Aiken *et al*. [15] observed a tendency to form more C-(N-)A-S-H and a decrease of porosity with increasing GGBFS fraction for fly ash/GGBFS-based AAMs, which led to a decreased neutralised (pH < 9) depth after sulfuric acid exposure. However, GGBFS addition led also to a more pronounced visible damage (exposure of aggregates), most likely through formation of gypsum.

In contrast to the above studies, the work of Sturm *et al*. [16] on silica/sodium aluminate-based AAMs indicated no positive effect of GGBFS (25 % addition) on sulfuric acid resistance; *viz*., the highest acid resistance was exhibited by the materials without GGBFS addition, and the depth of neutralisation (determined with phenolphthalein) was lowest for one of the materials without GGBFS. This was attributed to the fact that the formation of expansive gypsum was not observed in GGBFS-free materials, while gypsum was found in the GGBFS-containing materials, due to the differences in Ca content. Moreover, there are cases where formation of gypsum in GGBFS-based AAMs leads to the complete disintegration of samples [40], as mentioned earlier.

The addition of microsilica to metakaolin-based AAMs at a substitution rate of ≥7.5 % was found to increase their resistance against sulfuric acid attack, presumably due to an increased Si/Al ratio of the resulting K-A-S-H gel, and because the presence of additional SiO_2 led (by some not yet understood reaction mechanism) to a densified silica gel in the corroded layer [23]. Possibly related to this observation is the finding that silica/sodium aluminate-based AAMs performed better in sulfuric acid corrosion testing when they were designed with excess silica (rice husk ash or microsilica) [16]. Finally, of two metakaolin-based AAMs, the one with a lower water content and made from the metakaolin with a higher SiO_2 content (mainly due to a higher quartz content) performed better in a sewer environment (sulfuric acid attack), most likely because of a lower porosity and a finer pore structure [41].

Less data is available on the influence of AAM composition on the resistance against organic acids. However, in their study of the deterioration of AAMs in a mix of acetic, propionic and lactic acid, Koenig *et al*. [42] found that the acid resistance of AAMs, as measured by mass loss, residual compressive strength as well as depth of degradation, increased with decreasing GGBFS content, *i.e.*, the best performance was observed for the low-Ca AAM based on fly ash. Ukrainczyk [19] studied the complex interactions between metakaolin composition, the properties of the resulting materials (geopolymers) after activation with potassium silicate solution, and alkali leaching in acetic acid. Modelling indicated that the behaviour of the studied geopolymers depends mainly on their capacity to bind alkali ions, which in turn is influenced by the degree of the geopolymerisation reaction; in addition, crack formation and the porosity of the materials had an influence on their leaching resistance, as expected.

6 Additional properties

In several environments, e.g., in sewer systems and biogas plants, the acid that attacks the material is produced by microorganisms; in these cases, the combined process is often termed biodeterioration, biogenic acid corrosion (BAC) or microbially induced corrosion (MIC). Under MIC conditions, the deterioration rate is determined to a large degree by the colonisation by microorganisms and their activity [1, 2, 36, 37, 43]. While much research on conventional cement-based material has been conducted in this regard, only limited data pertaining to the effects of AAMs on the abundance and activity of microorganisms is available [41, 44, 45]; thus, additional studies are required to better understand this aspect. Further, because of the different processes involved, there may be differences between the behaviour of an AAM under MIC conditions and under the conditions of accelerated acid corrosion testing in the laboratory. For example, Khan *et al*. [17] found that a fly ash/GGBFS-based AAM exhibited very similar mass losses after 24 months of exposure to a sewer environment (*i.e.*, MIC conditions) and 6 months exposure to 1.5 % sulfuric acid solution (pH ≈ 0.8), but the depth to which the material was neutralised (pH < 10) was substantially higher when the samples were exposed to the sewer environment.

If AAMs are to be applied as repair materials for concrete structures in acid-exposed environments, they need to exhibit a sufficiently strong bond to the concrete substrate that is stable over the intended lifetime of the repair system. However, because of the significant differences between the chemical and mineralogical composition of low-Ca AAMs and conventional concretes, and because of the tendency of substantial shrinkage and associated cracking/spalling of high-Ca AAMs (alkali-activated slags) [46, 47], a strong and durable bond cannot be assumed *a priori*. Knowledge in this regard is only beginning to accumulate [48–51]; thus, additional studies, particularly considering the long-term behaviour of the bond, are required.

7 Research needs

From the above description of the current knowledge about the acid attack on AAMs, it follows that several open questions remain. These pertain to fundamental aspects of the deterioration process as well as to engineering aspects, such as optimum mix-design parameters.

Particularly for low-Ca AAMs, an important question is how the severe alkali leaching and neutralisation of the corroded layer, reaching to considerable depth, impacts their long-term chemical and mechanical stability, the protection of embedded steel reinforcement, and the bond to a substrate. Related to these questions are the decisions about how to define 'depth of corrosion' and 'acid resistance' of AAMs. Suitable and widely accepted definitions of these parameters are needed, as these would help to compare the results of different studies and, thus, to identify the influence of mix-design parameters on the acid resistance. Further, though it is obvious that a low permeability of the intact AAM will be beneficial for acid resistance in most instances, the relative importance of the transport properties of the intact material

and the corroded layer is unclear at present. Investigation of this issue will require dedicated analyses of the corroded layer itself, including porosity, mechanical and transport parameters (e.g., [42, 52–54]).

Multiple indications of congruent matrix dissolution and precipitation of silica gel in low-Ca AAMs have been presented in the literature. However, most of this evidence is circumstantial, and it would thus be highly desirable to obtain a definite proof of the proposed dissolution-reprecipitation mechanism, because only a reliable understanding of the deterioration mechanism will enable accurate modelling of acid attack and a well-informed design of new materials with high resistance. These investigations will require the application of appropriate spectroscopic methods to study the structural transformations of the aluminosilicate framework of the materials (e.g., [16, 22, 55]), and ideally also isotope methods that can be used to directly track dissolution and precipitation of the involved phases (e.g., [22, 31, 32, 56]). As for high-Ca and intermediate-Ca AAMs, the evidence regarding the mechanism of deterioration caused by acid attack is scarcer; thus, it should be investigated whether a dissolution-reprecipitation mechanism is operational also in these materials.

A further open question with potentially important implications is why, or whether, precipitation of gypsum (or other minerals) can clog cracks and decrease the permeability of certain AAMs, as has been claimed in an early publication [38], while it was found to be responsible for cracking, increased permeability and sometimes complete fragmentation in many other AAMs. Additional research requirements related to the interaction of microorganisms and AAMs under MIC conditions and regarding the bond between AAMs and a concrete substrate have been formulated in Section 6. Finally, a fine pore structure with predominantly small pores, which is the reason for the low permeability of alkali-activated slags, generally leads to substantial shrinkage and associated cracking [46, 47]. It should thus be investigated how shrinkage affects the acid resistance of these materials and their bond to concrete substrates, if used as repair material.

Acknowledgments

Authorship statement (CRediT)

Gregor J.G. Gluth: Conceptualization, Writing - original draft, Writing – review and editing, Visualization.

Cyrill Grengg, Neven Ukrainczyk, Florian Mittermayr, Martin Dietzel: Writing – review and editing.

References

[1] C. Grengg, F. Mittermayr, N. Ukrainczyk, G. Koraimann, S. Kienesberger, M. Dietzel, Advances in concrete materials for sewer systems affected by microbial induced concrete corrosion: a review, Water Res (2018) 134: 341-352. https://doi.org/10.1016/j.watres.2018.01.043

[2] M. Alexander, A. Bertron, N. De Belie (Eds.), Performance of Cement-Based Materials in Aggressive Aqueous Environments: State-of-the-Art Report, RILEM TC 211-PAE, Springer, 2013. https://doi.org/10.1007/978-94-007-5413-3

[3] J.L. Provis, S.A. Bernal, Geopolymers and related alkali-activated materials, Annu Rev Mater Res (2014) 44: 299-327. https://doi.org/10.1146/annurev-matsci-070813-113515

[4] J.L. Provis, J.S.J. van Deventer (Eds.), Alkali Activated Materials: State-of-the-Art Report, RILEM TC 224-AAM, Springer, 2014. https://doi.org/10.1007/978-94-007-7672-2

[5] J. Blaakmeer, Diabind: an alkali-activated slag fly ash binder for acid-resistant concrete, Adv Cem Based Mater (1994) 1: 275-276. https://doi.org/10.1016/1065-7355(94)90036-1

[6] A. Palomo, M.T. Blanco-Varela, M.L. Granizo, F. Puertas, T. Vazquez, M.W. Grutzeck, Chemical stability of cementitious materials based on metakaolin, Cem Concr Res (1999) 29: 997-1004. https://doi.org/10.1016/S0008-8846(99)00074-5

[7] C. Shi, J.A. Stegemann, Acid corrosion resistance of different cementing materials, Cem Concr Res (2000) 30: 803-808. https://doi.org/10.1016/S0008-8846(00)00234-9

[8] T. Bakharev, Resistance of geopolymer materials to acid attack, Cem Concr Res (2005) 35: 658-670. https://doi.org/10.1016/j.cemconres.2004.06.005

[9] A. Allahverdi, F. Škvára, Nitric acid attack on hardened paste of geopolymeric cement: Part 1, Ceram Silik (2001) 45: 81-88.

[10] A. Fernandez-Jimenez, I. García-Lodeiro, A. Palomo, Durability of alkali-activated fly ash cementitious materials, J Mater Sci (2007) 42: 3055-3065. https://doi.org/10.1007/s10853-006-0584-8

[11] C.W. Correns, W. von Engelhardt, Neue Untersuchungen über die Verwitterung des Kalifeldspates, Naturwissenschaften (1938) 26: 137-138. https://doi.org/10.1007/BF01772798

[12] E.H. Oelkers, General kinetic description of multioxide silicate mineral and glass dissolution, Geochim Cosmochim Acta (2001) 65: 3703-3719. https://doi.org/10.1016/S0016-7037(01)00710-4

[13] R.L. Hartman, H.S. Fogler, Understanding the dissolution of zeolites, Langmuir (2007) 23: 5477-5484. https://doi.org/10.1021/la063699g

[14] R.R. Lloyd, J.L. Provis, J.S.J. van Deventer, Acid resistance of inorganic polymer binders. 1. Corrosion rate, Mater Struct (2012) 45: 1-14. https://doi.org/10.1617/s11527-011-9744-7

[15] T.A. Aiken, J. Kwasny, W. Sha, M.N. Soutsos, Effect of slag content and activator dodage on the resistance of fly ash geopolymer binders to sulfuric acid attack, Cem Concr Res (2018) 111: 23-40. https://doi.org/10.1016/j.cemconres.2018.06.011

[16] P. Sturm, G.J.G. Gluth, C. Jäger, H.J.H. Brouwers, H.-C. Kühne, Sulfuric acid resistance of one-part alkali-activated mortars, Cem Concr Res (2018) 109: 54-63. https://doi.org/10.1016/j.cemconres.2018.04.009

[17] H.A. Khan, A. Castel, M.S.H. Khan, Corrosion of fly ash based geopolymer mortar in natural sewer environment and sulphuric acid solution, Corros Sci (2020) 168: 108586. https://doi.org/10.1016/j.corsci.2020.108586

[18] N. Ukrainczyk, O. Vogt, Geopolymer leaching in water and acetic acid, RILEM Tech Lett (2020) 5: 163-173. https://doi.org/10.21809/rilemtechlett.2020.124

[19] N. Ukrainczyk, Simple model for alkali leaching from geopolymers: effects of raw materials and acetic acid concentration on apparent diffusion coefficient, Materials (2021) 14: 1425. https://doi.org/10.3390/ma14061425

[20] O. Vogt, C. Ballschmiede, N. Ukrainczyk, E. Koenders, Evaluation of sulfuric acid-induced degradation of potassium silicate activated metakaolin geopolymers by semi-quantitative SEM-EDS analysis, Materials (2020) 13: 4522. https://doi.org/10.3390/ma13204522

[21] C. Grengg, N. Ukrainczyk, G. Koraimann, B. Mueller, M. Dietzel, F. Mittermayr, Long-term in situ performance of geopolymer, calcium aluminate and Portland cement-based materials exposed to microbially induced acid corrosion, Cem Concr Res (2020) 131: 106034. https://doi.org/10.1016/j.cemconres.2020.106034

[22] C. Grengg, G.J.G. Gluth, F. Mittermayr, N. Ukrainczyk, M. Bertmer, A. Guilherme Buzanich, M. Radtke, A. Leis, M. Dietzel, Deterioration mechanism of alkali-activated materials in sulfuric

acid and the influence of Cu: a micro-to-nano structural, elemental and stable isotopic multi-proxy study, Cem Concr Res (2021) 142: 106373. https://doi.org/10.1016/j.cemconres.2021.106373

[23] O. Vogt, N. Ukrainczyk, E. Koenders, Effect of silica fume on metakaolin geopolymers' sulfuric acid resistance, Materials (2021) 14: 5396. https://doi.org/10.3390/ma14185396

[24] R. Snellings, Solution-controlled dissolution of supplementary cementitious material glasses at pH 13: the effect of solution composition on glass dissolution rates, J Am Ceram Soc (2013) 96: 2467-2475. https://doi.org/10.1111/jace.12480

[25] N.M. Piatak, M.B. Parsons, R.R. Seal II, Characteristics and environmental aspects of slag: a review, Appl Geochem (2015) 57: 236-266. https://doi.org/10.1016/j.apgeochem.2014.04.009

[26] A. Allahverdi, F. Škvára, Nitric acid attack on hardened paste of geopolymeric cement: Part 2, Ceram Silik (2001) 45: 143-149.

[27] E. Lippmaa, M. Mägi, A. Samoson, G. Engelhardt, A.-R. Grimmer, Structural studies of silicates by solid-state high-resolution ^{29}Si NMR, J Am Chem Soc (1980) 102: 4889-4893. https://doi.org/10.1021/ja00535a008

[28] G.J.G. Gluth, P. Sturm, S. Greiser, C. Jäger, H.-C. Kühne, One-part geopolymers and aluminosilicate gel-zeolite composites based on silica: factors influencing microstructure and engineering properties, Ceram Eng Sci Proc (2019) 39(3): 183-196. https://doi.org/10.1002/9781119543381.ch17

[29] M. Dietzel, Dissolution of silicates and the stability of polysilicic acid, Geochim Cosmochim Acta (2000) 64: 3275-3281. https://doi.org/10.1016/S0016-7037(00)00426-9

[30] [30] R. Hellmann, R. Wirth, D. Daval, J.-P. Barnes, J.-M. Penisson, D. Tisserand, T. Epicier, B. Florin, R.L. Hervig, Unifying natural and laboratory chemical weathering with interfacial dissolution-reprecipitation: a study based on the nanometer-scale chemistry of fluid-silicate interfaces, Chem Geol (2012) 294-295: 203-216. https://doi.org/10.1016/j.chemgeo.2011.12.002

[31] T. Geisler, A. Janssen, D. Scheiter, T. Stephan, J. Berndt, A. Putnis, Aqueous corrosion of borosilicate glass under acidic conditions: a new corrosion mechanism, J Non-Cryst Solids (2010) 356: 1458-1465. https://doi.org/10.1016/j.jnoncrysol.2010.04.033

[32] T. Geisler, T. Nagel, M.R. Kilburn, A. Janssen, J.P. Icenhower, R.O.C. Fonseca, M. Grange, A.A. Nemchin, The mechanism of borosilicate glass corrosion revisited, Geochim Cosmochim Acta (2015) 158: 112-129. https://doi.org/10.1016/j.gca.2015.02.039

[33] A. Buvignier, C. Patapy, M. Peyre Lavigne, E. Paul, A. Bertron, Resistance to biodeterioration of aluminium-rich binders in sewer-network environment: study of the possible bacteriostatic effect and role of phase reactivity, Cem Concr Res (2019) 123: 105785. https://doi.org/10.1016/j.cemconres.2019.105785

[34] Y. Wang, Y. Cao, Z. Zhang, J. Huang, P. Zhang, Y. Ma, H. Wang, Study of acidic degradation of alkali-activated materials using synthetic C-(N)-A-S-H and N-A-S-H gels, Compos Part B (2022) 230: 109510. https://doi.org/10.1016/j.compositesb.2021.109510

[35] J. Ren, L. Zhang, B. Walkley, J.R. Black, R. San Nicolas, Degradation resistance of different cementitious materials to phosphoric acid attack at early stage, Cem Concr Res (2022) 151: 106606. https://doi.org/10.1016/j.cemconres.2021.106606

[36] A. Bertron, Understanding interactions between cementitious materials and microorganisms: a key to sustainable and safe concrete structures in various contexts, Mater Struct (2014) 47: 1787-1806. https://doi.org/10.1617/s11527-014-0433-1

[37] A. Bertron, M. Peyre Lavigne, C. Patapy, B. Erable, Biodeterioration of concrete in agricultural, agro-food and biogas plants: state of the art and challenges, RILEM Tech Lett (2017) 2: 83-89. https://doi.org/10.21809/rilemtechlett.2017.42

[38] A. Allahverdi, F. Škvára, Sulfuric acid attack on hardened paste of geopolymer cements: Part 1. Mechanism of corrosion at relatively high concentrations, Ceram Silik (2005) 49: 225-229.

[39] A. Allahverdi, F. Škvára, Sulfuric acid attack on hardened paste of geopolymer cements: Part 2. Corrosion mechanism at mild and relatively low concentrations, Ceram Silik (2006) 50: 1-4.

[40] J. Aliques-Granero, T.M. Tognonvi, A. Tagnit-Hamou, Durability test methods and their application to AAMs: case of sulfuric-acid resistance, Mater Struct (2017) 50: 36. https://doi.org/10.1617/s11527-016-0904-7

[41] C. Grengg, G. Koraimann, N. Ukrainczyk, O. Rudic, S. Luschnig, G.J.G. Gluth, M. Radtke, M. Dietzel, F. Mittermayr, Cu- and Zn-doped alkali activated mortar - properties and durability in (bio)chemically aggressive wastewater environments, Cem Concr Res (2021) 149: 106541. https://doi.org/10.1016/j.cemconres.2021.106541

[42] A. Koenig, A. Herrmann, S. Overmann, F. Dehn, Resistance of alkali-activated binders to organic acid attack: assessment of evaluation criteria and damage mechanisms, Constr Build Mater (2017) 151: 405-413. https://doi.org/10.1016/j.conbuildmat.2017.06.117

[43] C. Grengg, F. Mittermayr, G. Koraimann, F. Konrad, M. Szabó, A. Demeny, M. Dietzel, The decisive role of acidophilic bacteria in concrete sewer networks: a new model for fast progressing microbial concrete corrosion, Cem Concr Res (2017) 101: 93-101. https://doi.org/10.1016/j.cemconres.2017.08.020

[44] B. Drugă, N. Ukrainczyk, K. Weise, E. Koenders, S. Lackner, Interaction between wastewater microorganisms and geopolymer or cementititous materials: biofilm characterization and deterioration characterisitics of mortars, Int Biodeterior Biodegrad (2018) 134: 58-67. https://doi.org/10.1016/j.ibiod.2018.08.005

[45] M. Giroudon, M. Peyre Lavigne, C. Patapy, A. Bertron, Blast-furnace slag cement and metakaolin based geopolymer as construction materials for liquid anaerobic digestion structures: interactions and biodeterioration mechanisms, Sci Total Environ (2021) 750: 141518. https://doi.org/10.1016/j.scitotenv.2020.141518

[46] S.A. Bernal, J. Bisschop, J.S.J. van Deventer, J.L. Provis, Drying shrinkage microcracking of alkali-activated slag materials, Proceedings of the 34th Annual Cement and Concrete Science Conference, and Workshop on Waste Cementation, S.A. Bernal, J.L. Provis (Eds.), 2014, 59-62.

[47] C. Cartwright, F. Rajabipour, A. Radlińska, Shrinkage characteristics of alkali-activated slag cements, J Mater Civ Eng (2015) 27: B4014007. https://doi.org/10.1061/(ASCE)MT.1943-5533.0001058

[48] V.A. Nunes, P.H.R. Borges, C. Zanotti, Mechanical compatibility and adhesion between alkali-activated repair mortars and Portland cement concrete substrate, Constr Build Mater (2019) 215: 569-581. https://doi.org/10.1016/j.conbuildmat.2019.04.189

[49] P. Sturm, G.J.G. Gluth, H.J.H. Brouwers, H.-C. Kühne, Shrinkage and bond behaviour of one-part alkali-activated mortars, Proceedings of the International Conference on Sustainable Materials, Systems and Structures (SMSS 2019) - Vol. 3: Durability, Monitoring and Repair of Structures, A. Barčević, M.J. Rukavina, D. Damjanović, M. Guadagnini (Eds.), RILEM Publications, 2019, 103-110.

[50] J. Juhart, C. Gößler, C. Grengg, F. Mittermayr, O. Rudic, A. McIntosh, B. Freytag, Material characterization of geopolymer mortar for its beneficial use in composite construction, RILEM Tech Lett (2020) 5: 174-185. https://doi.org/10.21809/rilemtechlett.2020.125

[51] Y.-S. Wang, K.-D. Peng, A. Alrefaei, J.-G. Dai, The bond between geopolymer repair mortars and OPC concrete substrate: strength and microscopic interactions, Cem Concr Compos (2021) 119: 103991. https://doi.org/10.1016/j.cemconcomp.2021.103991

[52] Y.F. Houst, F.H. Wittmann, Influence of porosity and water content on the diffusivity of CO_2 and O_2 through hydrated cement paste, Cem Concr Res (1994) 24: 1165-1176. https://doi.org/10.1016/0008-8846(94)90040-X

[53] A. Leemann, R. Loser, B. Münch, P. Lura, Steady-state O_2 and CO_2 diffusion in carbonated mortars produced with blended cements, Mater Struct (2017) 50: 247. https://doi.org/10.1617/s11527-017-1118-3

[54] B. Wild, D. Daval, J.-S. Micha, I.C. Bourg, C.E. White, A. Fernandez-Martinez, Physical properties of interfacial layers developed on weathered silicates: a case study based on labradorite feldspar, J Phys Chem C (2019) 123: 24520-24532. https://doi.org/10.1021/acs.jpcc.9b05491

[55] C. Lenting, T. Geisler, Corrosion of ternary borosilicate glass in acidic solution studied in operando by fluid-cell Raman spectroscopy, npj Mater Degrad (2021) 5: 37. https://doi.org/10.1038/s41529-021-00182-5

[56] F.M. Stamm, T. Zambardi, J. Chmeleff, J. Schott, F. von Blanckenburg, E.H. Oelkers, The experimental determination of equilibrium Si isotope fractionation factors among $H_4SiO_4^0$, $H_3SiO_4^-$ and amorphous silica ($SiO_2 \cdot 0.32\ H_2O$) at 25 and 75 °C using the three-isotope method, Geochim Cosmochim Acta (2019) 255: 49-68. https://doi.org/10.1016/j.gca.2019.03.035

[57] C. Montes, E.N. Allouche, Evaluation of the potential of geopolymer mortar in the rehabilitation of buried infrastructure, Struct Infrastruct Eng (2012) 8: 89-98. https://doi.org/10.1080/15732470903329314

[58] S.A. Bernal, E.D. Rodríguez, R. Mejía de Gutiérrez, J.L. Provis, Performance of alkali-activated slag mortars exposed to acids, J Sustain Cem Based Mater (2012) 1: 138-151. https://doi.org/10.1080/21650373.2012.747235

[59]   Z. Li, S. Peethamparan, Leaching resistance of alkali-activated slag and fly ash mortars exposed to organic acid, Green Mater (2018) 6: 117-130. https://doi.org/10.1680/jgrma.18.00021

[60]   N. Ukrainczyk, M. Muthu, O. Vogt, E. Koenders, Geopolymer, calcium aluminate, and Portland cement-based mortars: comparing degradation using acetic acid, Materials (2019) 12: 3115. https://doi.org/10.3390/ma12193115

[61]   D.A. Kulik, T. Wagner, S.V. Dmytrieva, G. Kosakowski, F.F. Hingerl, K.V. Chudnenko, U. Berner, GEM-Selektor geochemical modeling package: revised algorithm and GEMS3K numerical kernel for coupled simulation codes. Comput Geosci (2013) 17: 1-24. https://doi.org/10.1007/s10596-012-9310-6

[62]   T. Wagner, D.A. Kulik, F.F. Hingerl, S.V. Dmytrieva, GEM-Selektor geochemical modeling package: TSolMod library and data interface for multicomponent phase models. Can Mineral (2012) 50: 1173-1195. https://doi.org/10.3749/canmin.50.5.1173

[63]   B. Lothenbach, D.A. Kulik, T. Matschei, M. Balonis, L. Baquerizo, B. Dilnesa, G.D. Miron, R.J. Myers, Cemdata18: a chemical thermodynamic database for hydrated Portland cements and alkali-activated materials, Cem Concr Res (2019) 115: 472-506. https://doi.org/10.1016/j.cemconres.2018.04.018